

INVESTIGATIONS OF ADDITIONAL LOSSES IN SUPERCONDUCTING NIOBIUM CAVITIES DUE TO FROZEN-IN FLUX

B. Piosczyk, P. Kneisel, O. Stoltz, J. Halbritter
Kernforschungszentrum und Universität Karlsruhe
Germany

Summary

Measurements of the additional losses due to frozen-in magnetic flux have been carried out between 80 and 413 MHz and 2 and 5 GHz. In difference to the results in the GHz-region a not expected stronger temperature and rf-field dependence occurred in the 100 MHz region.

I. Introduction

Among the mechanisms yielding rf residual losses only one can be studied easily today: namely the influence of frozen-in magnetic flux, because the amount of flux can be varied systematically. The variation of flux is achieved by applying an external dc field H_{dc} above T_c and then cooling the cavity below T_c .¹⁻⁴ With our high Q_0 cavities we are able to measure losses due to a small number of fluxoid accurately, which is not only important for the application of superconducting cavities, e.g. in accelerators, but also gives some insight into the dynamics of nearly independent fluxoids.

These additional losses due to frozen-in flux can be described by a surface resistance R_H , which has been observed to be proportional to H_{dc} ($< H_c/100$) and roughly to the surface resistance R_{NL} of the normal state.¹⁻⁵ The frequency dependence given by $R_{NL} \propto f^\alpha$ ($1/2 < \alpha < 2/3$) is slower than that of the superconducting part $R_s \propto f^\alpha$ ($\alpha \approx 1.6$).⁶ Therefore fluxoid losses become more important at lower frequencies; moreover low frequency cavities are larger and hence suffer more from fluxoids generated by thermoelectric currents.^{1,7} On the other side in low frequency cavities the residual losses are always increasing with rf field level^{8,9} in contrast to GHz cavities. These observations led us to study R_H systematically as function of temperature T , rf field level H_p and frequency f in superconducting helices¹⁰ (0,1-0,4 GHz) and cavities (2-5 GHz) in order to identify fluxoid losses. Whereas the results around 3 GHz have been measured and explained before,¹ the results observed with the helical cavity have not been reported so far.

II. Experimental Arrangements and Results

a) S-band-cavity

The measurements between 2 and 5 GHz have been carried out in a cylindrical (height=diameter=2r=10 cm) solid niobium cavity, as described in¹⁰. The cavity was placed in the field B_{dc} of a coil wound on a coaxial cylinder around the cavity; this whole setup was shielded to less than 10 mOe. The homogeneity of the field over the cavity volume was about 5%. Above T_c the external field H_{dc} was applied by energizing

the coil. In cooling to T_c the cylinder walls become superconducting first thus enclosing a flux $B_{dc} \cdot A$, with $A=r^2 \cdot \pi$ the area of the cavity. The endplates become superconducting when in cooling $B_{c2}(T)$ approaches B_{dc} , because Nb is a Type II superconductor (Ginzburg-Landau parameter $K_{GL} = 0.8$).¹¹ This freezing-in of flux in the endplates was proved by two Hall probes placed at one end plate of the cavity in the center and at about 0.6r which showed that the flux was trapped mainly in the region $\leq 0.6r$ of the endplates. Therefore we choose for the investigation of additional losses due to B_{dc} the mode family TM_{01p} ($p=0,1,2,3$), all of which have the same spatial field distribution across the endplates. The partial geometry factors G_p for the endplates can be calculated¹ and is for the TM_{010} mode three times, in the other TM_{01p} modes two times the geometry factor G of the whole cavity.

The investigation consisted in measuring the temperature dependence of the surface resistance in the different modes at applied fields of 0.5, 1, 3 and 5 Oe at small rf field levels ($H_p < 5$ Oe). The measurements with $H_{dc} \neq 0$ were bracketed by two measurements with $H_{dc} = 0$. The Q -values for the TM_{01p} modes ($H_{dc} = 0$) were in 10^{10} -range. In addition the dependence on rf field level H_p has been measured at 1.4 K for $H_{dc} = 0.5$ and 1 Oe.

The evaluation of the experimental data took place by taking the differences of the Q -values with and without frozen-in flux. Together with the partial geometry factor this yields the additional surface resistance

$$R_H(H_{dc}, H_p, f, T) = G_p \left\{ \frac{1}{Q(H_{dc})} - \frac{1}{Q(H_{dc}=0)} \right\}$$

where $Q(H_{dc})$ is the measured Q -value with frozen-in magnetic field H_{dc} , G_p is the partial geometry factor.

We found a temperature dependence of R_H which can be described by

$$R_H(T) = \frac{H_{dc}}{H_c(0)} \cdot \frac{R_{NL}}{\gamma} \frac{1}{1 - (T/T_c)^2} \quad (1)$$

as shown in Fig. 1 for the TM_{010} -mode. $H_c(0) = 1980$ Oe is the thermodynamical critical magnetic field of niobium at $T=0$, $T_c=9.25$ K its critical temperature. R_H depends linear on H_{dc} . Fig. 2 shows a frequency dependence

$$R_H(f) \propto f^\alpha \quad \alpha = 0.5 \quad (2)$$

$\alpha = 0.5$ is a mean value of several runs, where α -values between 0.4 and 0.6 have been obtained. In using $R^* = R_{NL}/\gamma$, R_{NL} (3 GHz, 0.3 μ cm) = $5 \times 10^{-3} \Omega$, which was calculated with the measured bulk resistance¹² and agrees with the rf measurements¹³, we obtain $\gamma \approx 1$.

In agreement with other measurements^{1,14} we did not find any increasing of R_H with rf field up to $H_p \approx 150$ Gauss.

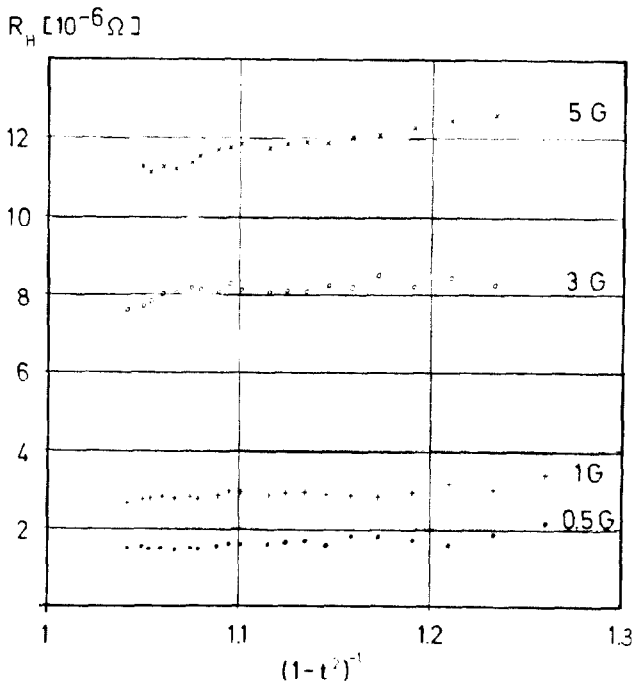


Fig. 1. Temperature dependence of the additional losses R_H due to frozen-in magnetic flux at applied dc-fields of 0.5, 1, 3 and 5 Gauss. The data are taken in the TM_{010} -mode at 2.17 GHz.

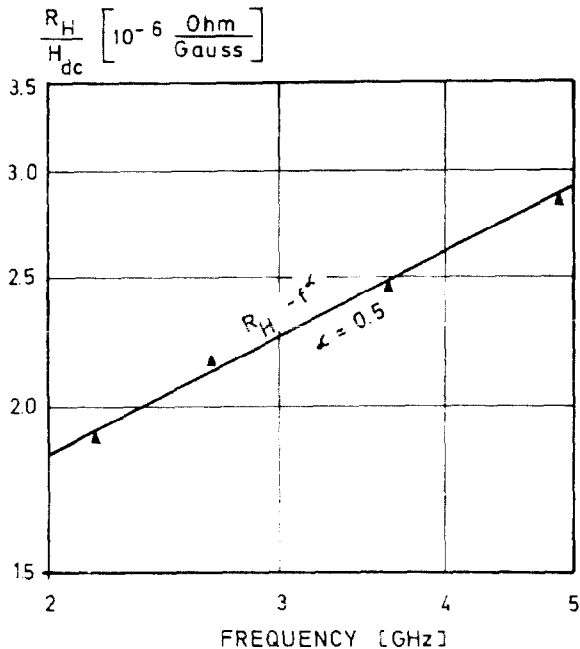


Fig. 2. The frequency dependence of the additional losses R_H .

b) Helical cavities

For the measurements of R_H between 80 and 400 MHz we used cavities loaded with a helically wound Nb-tube of about 3 m length and 0.63 cm (helix I) or 0.8 cm (helix II) outer

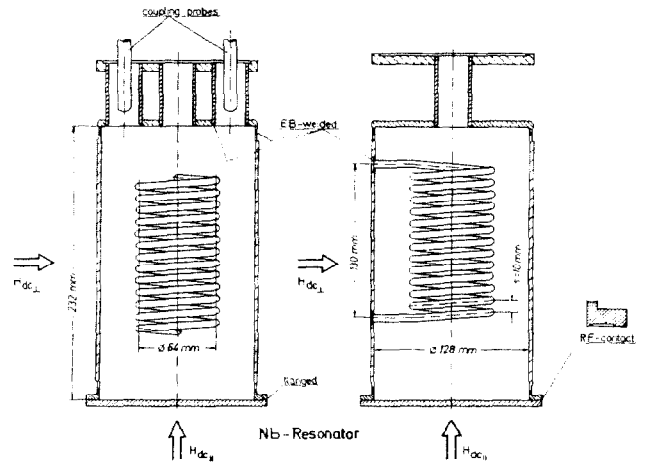


Fig. 3. Helically loaded Nb-cavity. The applied external dc-field H_{dc} was parallel and perpendicular to the axes.

diameter (Fig. 3). The helices were welded into a Nb-can, with welded top plates whereas the bottom plate was either top welded (helix I) or flanged (helix II). Both helices were stress annealed, chemically (helix I) or electrochemically (helix II) polished and anodized ($\approx 400 \text{ \AA}$ Nb_2O_5)^{8,10} for protection. For helix I we measured the harmonics between $f=80$ MHz and $f=305$ MHz, for helix II between $f=91$ MHz and $f=413$ MHz. The geometry factor G was between 4 and 8 Ω . The rf peak field H_p is given approximately by $H_p [\text{Gauss}] \approx 0.07 \cdot \sqrt{PQ} [\text{Watt}]$. P is the dissipated power in the cavity.

The geometry factors G were determined by measuring the Q -values at room temperature and using the known normal surface resistance R_{NL} : $G = Q \cdot R_{NL}$. The peak fields were calculated both with the ring model¹⁵ and with a model using conformal transformations.¹⁶

The earth magnetic field was shielded to less than 10 mOe. With two coils inside the shielding cylinder the external field H_{dc} was produced, either parallel ($H_{dc\parallel}$) or perpendicular ($H_{dc\perp}$) to the axis of the helix. The homogeneity of H_{dc} over the volume of the cavity was for $H_{dc\parallel}$ about 5%, but at $H_{dc\perp}$ a component of $H_{dc\parallel}$ up to 20% has been measured inside the cavity volume. Measurements with $H_{dc} \neq 0$ were bracketed by measurements with $H_{dc} = 0$. To get R_H out of the measured $Q(H_{dc})$ we used the formula $R_H = G [1/Q(H_{dc}) - 1/Q(0)]$, with the total geometry factor G . For the correct R_H we would have to use the unknown partial geometry factor G_p , which takes into account the non homogeneous distribution of the fluxoids and rf fields over the surface.

$R_H(H_{dc})$ is roughly proportional to the applied field, $R_H(H_{dc}) \approx H_{dc}$, which we have proved up to $H_{dc} \approx 6$ Gauss. At low rf fields ($H_p \leq 5$ Gauss) R_H is independent of H_p . In this case the temperature and frequency dependence (Fig. 4) can be described by:

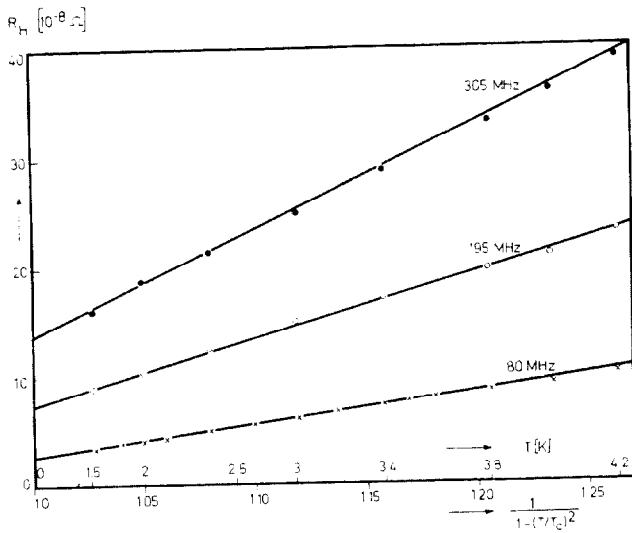


Fig. 4. Additional resistance R_H at low rf-fields as a function of T at $H_{dc\parallel} = 6$ Gauss for different modes at helix I.

$$R_H(T, f) = \frac{H_{dc}}{H_c(0)} \cdot \frac{R_{NL}}{\gamma(f)} \cdot \frac{1+r_T(f) \left(\frac{T}{T_c}\right)^2}{1+(T/T_c)^2} \quad (3)$$

$$\text{with } \gamma(f) = \gamma \cdot (100 \text{ MHz}/f)^\alpha;$$

$$r_T(f) = r_T \cdot (100 \text{ MHz}/f)^\beta.$$

For R_{NL} ($\approx f \cdot 0.5$) we use the measured mean free path of about 300 \AA , yielding $R_{Nb}(80 \text{ MHz}, 1.6 \text{ } \mu\text{cm}) \approx 2.3 \cdot 10^{-3} \Omega$. For the two helical cavities we got:

| | Helix I | | Helix II | |
|----------|-------------------|---------------|-------------------|---------------|
| | $H_{dc\parallel}$ | $H_{dc\perp}$ | $H_{dc\parallel}$ | $H_{dc\perp}$ |
| γ | 190 | 230 | 150 | 110 |
| α | 1.4 | 0.75 | 1.3 | 0.8 |
| r_T | 10 | 10 | 13 | 13 |
| β | 0.4 | 0.4 | 0.7 | 0.7 |

α and γ depend on the orientation of H_{dc} relative to the helix because of the different frequency dependence of the partial geometry factor for either field direction. The larger γ -values for helix I could be due to thinner helix tube, whereas the differences in the ratio $\gamma(H_{dc\parallel})/\gamma(H_{dc\perp})$ of both helices may be due to uncertainties in the distribution of H_{dc} . In contrast to the results in the GHz-region the additional losses in the 100 MHz region increase stronger with temperature. In Eq. (3) this is represented by the second term $r_T(f)$. But Nb helices show not only more complicated temperature dependencies but also unforeseen dependencies on surface peak field H_p (Fig. 5) which can be represented by:

$$R_H(H_p, T, f) = R_H(0, T, f) [1+r_H(T, f)(H_p/H_c(0))^\delta] \quad (4)$$

with $\delta=1$ for $H_p \leq 100$ Gauss and $0.5 \leq \delta < 1$ for $100 \text{ Gauss} \leq H_p \leq 600$ Gauss. $R_H(0, T, f)$ is the low field value as given by Eq. (3). The increase of R_H with H_p is decreasing with frequency. This is roughly given by $R_H \propto 1/f^{1-2}$ (Fig. 6). Because we have measured the H_p dependence for 1.4 K and 4.2 K only, we cannot fit a function to $r_H(T, f)$; but $r_H(T, f)$ at 4.2 K is smaller than at 1.4 K by about a factor of 3 at 91.4 MHz. $r_T(f)$ and $r_H(T, f)$ don't depend on

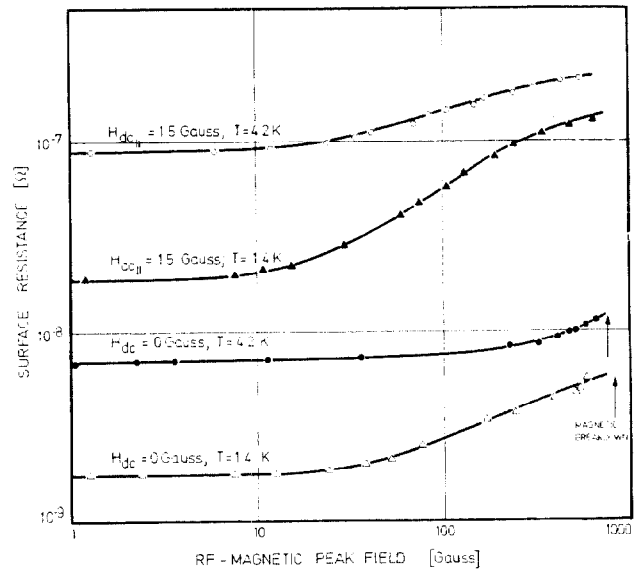


Fig. 5. The dependence of the surface resistance on rf-field amplitude with $H_{dc} = 0$ and $H_{dc\parallel} = 1.5$ Gauss for helix II at $f = 91.4$ MHz.

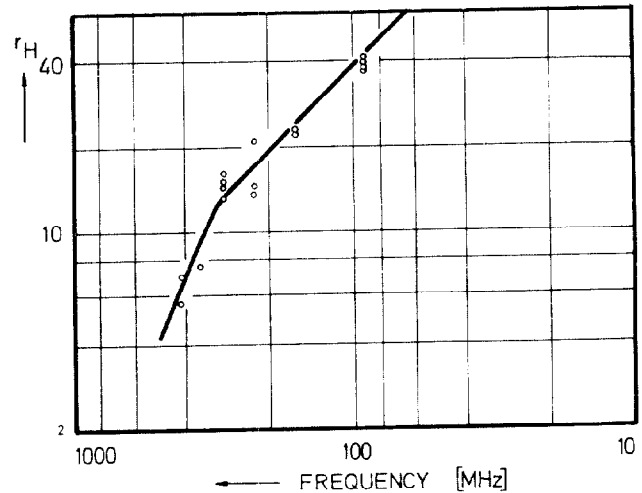


Fig. 6. $r_H(f, T)$ as a function of frequency at $T = 1.4$ K for external dc-fields parallel and perpendicular to the helix axis for helix II.

the orientation of H_{dc} . This is due to the fact that in contrast to α and γ which include the unknown partial geometry factor, $r_T(f)$ and $r_H(T, f)$ are relative values independent of the used geometry factor and depend therefore only on material properties which are different for both helices. The parts of R_H represented by $r_T(f)$ and $r_H(f, T)$ are thought to be caused by oscillating of the fluxoids in the rf field.

Summarizing the helix results mainly in their difference to the GHz results: In the 100 MHz region the losses increase stronger with temperature and as a new dependence an increase with rf amplitude appears.

III. Discussion

As we mentioned in Part IIa, cooling a Type II superconductor in a magnetic field

B_{dc} yields the phase transition to the superconducting fluxoid phase at $B_{dc} = B_{c2}(T)$, i.e. $T < T_c$. The flux frozen in this transition is given by $B_{dc} \cdot A$, where A is the area enclosed by extended Nb walls parallel to H_{dc} ; if the extension of walls parallel to H_{dc} is comparable to diameters of A , some flux will be excluded because of a demagnetization factor < 1 . This is possibly the reason why for helices (Part. IIb) and cavities with beam hole¹⁴ R_H is smaller than in cylindrical cavities (Part. IIa), in parallel fields. It should be mentioned, that also in Type I superconductors, flux can be frozen in as fluxoids. This happens in Pb plated ($\leq 10 \mu$) copper cavities,^{1,17} because the coherence length $\xi_{GL}(T)$ at $B_{dc} = B_c(T)$ was comparable to the thickness of the Pb plating. So that in R_H -experiments in high Q_0 cavities we have to deal only with losses due to fluxoids. Losses due to fluxoids are not well understood even at low frequencies,¹⁸ therefore we will mention only shortly some models. Absorption is governed by the density of states hence the enhanced losses due to fluxoids will depend on the low lying states inside the gap. In pure materials these localized states are equally spaced by Δ^2/E_F (Δ =gap parameter, E_F = Fermi energy),¹⁹ which for Nb correspond to a frequency of about 30 MHz. Therefore in pure Nb, i.e. mean free path longer than coherence length corresponding to $RRR < 10$, a frequency of 30 MHz will separate different regimes of absorption behaviours.

In the GHz region ($\gg 30$ MHz) transitions between neighbouring states like in the normal conducting state will dominate the absorption, hence the absorption can be described by rf shielding currents driven through the "quasinormal cores" of fluxoids. That is the absorption will scale like the core area

$$R_H = \frac{H_{dc}}{H_c(0)} \cdot R^* \cdot \frac{1}{1 - (T/T_c)^2}$$

and will be independent on rf amplitude.¹⁴ The surface resistance depends on the transition matrix elements and is of the same order and has the same frequency dependence as $R_{NL} (\propto f^\alpha, 0.5 < \alpha < 0.7, \text{ see Fig. 2 and } 1^{1-3,5})$. Therefore, R^* is usually identified by $R^* = R_{NL}/\gamma$ with a fit factor γ . The value of $\gamma \approx 1$, which we have measured at S-band, is in surprisingly good agreement with the model of "quasinormal cores" compared to $\gamma \approx 3$ observed earlier^{1,3}. We would like to point out that the material dependence thought of by the use of R_{NL} , was not proved and will be approximately true only for dirty materials, where the localized states are smeared out enough.⁵ For clean materials this is not clear, as shown by the factor 3 difference between R_H described in^{1,3} and in this paper. Hence the only important and understood and measured feature of the above model, Eq. (1) is the temperature dependence and the independence on rf amplitudes in the GHz region. For dirtier materials the above model seems to be valid also for lower frequencies,² whereas our helix measurements show major deviations in T, f and H_0 dependence. Because the motion of fluxoids is caused by the amplitude dependent Lorentz force²¹ the observed amplitude dependence [Eq. (4) and Fig. 5] reflects the non-linear motion.

The speed of fluxoids is limited by the possibility to dissipate the kinetic energies of the currents. Therefore the oscillation will disappear with increasing frequency, which we have observed by the decrease of r_T and r_H , above 80 MHz indicating a relaxation time for fluxoid oscillations above 10^{-8} sec.

Summarizing the above models: In pure Nb ($RRR \geq 10$) the level spacing of low lying states localized at the fluxoid core is around 30 MHz.¹⁹ Therefore around 30 MHz the temperature and frequency dependence will be stronger than around 3 GHz ($\gg 30$ MHz), where $R_H \approx R_{NL} \cdot H_{dc}/H_c(T)$ holds. The motion (oscillation) yields the amplitude dependent losses $R_H \approx (1 + r_H H_0^2)$ ($0.5 \leq \delta \leq 1$) around 100 MHz. These oscillations disappear above the relaxation time which is given by the possibility of slowing down the currents by dissipation.

IV. Conclusions

The additional surface resistance R_H due to frozen-in flux differs in the both examined frequency regions. In the GHz-region the behaviour can be described quantitatively by a model of "quasinormal cores", Eq. (1). In the low frequency region the behaviour of R_H is more complicated. As results the temperature dependence of R_H is stronger, Eq. (3), and there occurs an increase of R_H with rf surface field, Eq. (4). The difference to the GHz region may be caused by oscillating fluxoid in the rf-field.

For practical application the limitations set by earth field (≈ 0.5 Gauss) are of interest. We quote the following figures which are valid for $H_{dc} \approx 0.5$ Gauss and $T = 1.4$ K:

- 1) $R_H \approx 10^{-6} \Omega$ for any rf-field H_p at 3 GHz
- 2) $R_H \approx 0.25 \cdot 10^{-8} \Omega$ for low rf-field at 80 MHz
- 3) $R_H \approx 1.9 \cdot 10^{-8} \Omega$ for rf-field $H_p \approx 500$ Gauss at 80 MHz

This means that for applications at higher rf-fields the shielding of low frequency structures has to be more careful as one would expect from measurements of R_H at low rf-fields⁴.

References

- 1) J.M. Pierce, thesis (Stanford Univ. 1967)
J. Halbritter, K. Hoffmann, Proc. of the 1966 Lin. Acc. Conf., Los Alamos, 1966, p. 499
- 2) C.R. Haden, W.H. Hartwig, Phys. Rev. **148**, 313 (1966). J.M. Victor, W.H. Hartwig, J. Appl. Phys. **39**, 2539 (1968)
- 3) P. Kneisel, O. Stoltz, J. Halbritter, IEEE Trans. NS-18, No. 3, 159 (1971)
- 4) J.E. Vetter et al., Proc. of the 1970 Proton Lin. Acc. Conf., Batavia, p. 249
- 5) e.g. B. Rosenblum, M. Cordona, G. Fischer, RCA Review **25**, 491 (1964); J. le G. Gilchrist, P. Monceau, Phil. Mag. **18**, 237 (1968)
- 6) e.g. J. Halbritter, Z. Phys., **238**, 466 (1970),
- 7) Ch. Jones, J. Judish, NAL Oak Ridge, private communication
- 8) A. Citron et al., Proc. 8th Intern. High Energy Acc. Conf., Geneva, 1971, p. 276; J.E. Vetter, B. Piosczyk, J.L. Fricke, Proc. Proton Lin. Acc. Conf., Los Alamos 1972, p. 145; R. Benaroya et al., Appl. Phys. Lett. **21**, 235 (1972)
- 9) I. Ben Zvi, J.G. Castle, P.H. Ceperly, IEEE Trans. NS-19, No. 2, 226 (1972)
- 10) P. Kneisel, thesis (University Karlsruhe, 1972)

- 11) J. Halbritter, Externer Bericht 3/72-3 (KFZ, Karlsruhe, 1972)
- 12) P. Kneisel, O. Stoltz, J. Halbritter, this conf.
- 13) H. Hahn, H.J. Halama, IEEE Trans. NS-16, No. 3, 1013 (1969)
- 14) W. Bauer et al., this conf.
- 15) O. Siart, thesis (Universität Frankfurt, 1971)
- 16) A.J. Sierk, C.J. Hamer, T.A. Tombrello, Part. Acc. 2, 149, (1971)
- 17) M. Tinkham, Phys. Rev. 129, 2413 (1963)
- 18) P.H. Melville, Advances in Phys. 21 (1972) p. 647
- 19) C. Caroli, P.G. De Gennes, J. Matricon; Phys. Lett. 9, 4, 1964, (307)
- 20) F. Irie, K. Yamafui, J. Phys. Soc. Japan, 23, 2, 1966 (255)